

MIT Open Access Articles

X-Hair: 3D Printing Hair-like Structures with Multi-form, Multi-property and Multi-function

The MIT Faculty has made this article openly available. **Please share** how this access benefits you. Your story matters.

Citation: Wang, Guanyun, Ji, Junzhe, Xu, Yunkai, Ren, Lei, Wu, Xiaoyang et al. 2024. "X-Hair: 3D Printing Hair-like Structures with Multi-form, Multi-property and Multi-function."

As Published: <https://doi.org/10.1145/3654777.3676360>

Publisher: ACM|The 37th Annual ACM Symposium on User Interface Software and Technology

Persistent URL: <https://hdl.handle.net/1721.1/157555>

Version: Final published version: final published article, as it appeared in a journal, conference proceedings, or other formally published context

Terms of Use: Article is made available in accordance with the publisher's policy and may be subject to US copyright law. Please refer to the publisher's site for terms of use.



X-Hair: 3D Printing Hair-like Structures with Multi-form, Multi-property and Multi-function

Guanyun Wang
Zhejiang University
Hangzhou, China
guanyun@zju.edu.cn

Lei Ren
Zhejiang University
Hangzhou, China
renlei_design@zju.edu.cn

Xiaojing Zhou
Zhejiang University
Hangzhou, China
xiaojingzhou@zju.edu.cn

Lingyun Sun
Zhejiang University
Hangzhou, China
sunly@zju.edu.cn

Junzhe Ji
Zhejiang University
Hangzhou, China
jjunzhe@zju.edu.cn

Xiaoyang Wu
Zhejiang University
Hangzhou, China
churchillwoo@zju.edu.cn

Xin Tang
Hangzhou City University
Hangzhou, China
sophiatang0709@gmail.com

Ye Tao*
Hangzhou City University
Hangzhou, China
taoye@hzcu.edu.cn

Yunkai Xu
Zhejiang University
Hangzhou, China
liyexu09@gmail.com

Chunyuang Zheng
Zhejiang University
Hangzhou, China
3200103594@zju.edu.cn

Boyu Feng
Zhejiang University
Hangzhou, China
boyufeng@zju.edu.cn

Jiaji Li*
CSAIL, MIT
Cambridge, United States
jiaji@mit.edu



Figure 1: Examples of X-Hair applications: (a) Feather, (b) Dandelion, (c) Stanford Bunny, (d) Wig, (e) Brush, (f) Hairy Lamp. Scale Bar: 20mm.

ABSTRACT

In this paper, we present X-Hair, a method that enables 3D-printed hair with various forms, properties, and functions. We developed a two-step suspend printing strategy to fabricate hair-like structures in different forms (e.g. fluff, bristle, barb) by adjusting parameters including Extrusion Length Ratio and Total Length. Moreover, a design tool is also established for users to customize hair-like structures with various properties (e.g. pointy, stiff, soft) on imported 3D

models, which virtually shows the results for previewing and generates G-code files for 3D printing. We demonstrate the design space of X-Hair and evaluate the properties of them with different parameters. Through a series of applications with hair-like structures, we validate X-hair's practical usage of biomimicry, decoration, heat preservation, adhesion, and haptic interaction.

CCS CONCEPTS

• Human-centered computing → Interactive system and tools.

KEYWORDS

3D Printing, Personal Fabrication, Computer-Aided Design

ACM Reference Format:

Guanyun Wang, Junzhe Ji, Yunkai Xu, Lei Ren, Xiaoyang Wu, Chunyuang Zheng, Xiaojing Zhou, Xin Tang, Boyu Feng, Lingyun Sun, Ye Tao, and Jiaji Li. 2024. X-Hair: 3D Printing Hair-like Structures with Multi-form, Multi-property and Multi-function. In *The 37th Annual ACM Symposium on User Interface Software and Technology (UIST '24)*, October 13–16, 2024, Pittsburgh, PA, USA. ACM, New York, NY, USA, 14 pages. <https://doi.org/10.1145/3654777.3676360>

*Corresponding Authors.

Permission to make digital or hard copies of all or part of this work for personal or classroom use is granted without fee provided that copies are not made or distributed for profit or commercial advantage and that copies bear this notice and the full citation on the first page. Copyrights for components of this work owned by others than the author(s) must be honored. Abstracting with credit is permitted. To copy otherwise, or republish, to post on servers or to redistribute to lists, requires prior specific permission and/or a fee. Request permissions from permissions@acm.org.
UIST '24, October 13–16, 2024, Pittsburgh, PA, USA

© 2024 Copyright held by the owner/author(s). Publication rights licensed to ACM.
ACM ISBN 979-8-4007-0628-8/24/10
<https://doi.org/10.1145/3654777.3676360>

1 INTRODUCTION

Hair-like structures widely exist in nature, from the flagellum of sperm cells for swimming to the feathers of birds for flight, from the fluff on dandelion seeds to the woolly fur of mammoths. Multi-materials, multi-forms, and multi-functional hair-like structures are precisely adapted to their ecological functions. With the development of personal fabrication devices and technologies, 3D printing increasingly provides greater accuracy in customization. Therefore, we see an opportunity to explore 3D printed hair-like structures, which have existed for a long history but have not fully been explored in the field of the Human-Computer Interaction (HCI) community.

In recent years, HCI researchers have been constantly focusing on 3D-printed hair-like structures to explore their external or functional usages in interactive objects. 3D Printed Hair [14] first realized homogeneous hair-like structures printed by FDM (Fused Deposition Modeling) printer. Cillia [22] uses DLP (Digital Light Processing) printers to achieve micro and fine hair-like structures for motion conduction and aesthetic appearance. To further enhance the flexibility of the printing process and realize more kinds of prototypes with hair-like structures, Extruder-Turtle [26] provides a geometry library which helps to generate G-code files to print on FDM printers. Generally, previous works attempt to fabricate hair-like structures with single and uniform properties based on conventional printing methods, while hair-like structures with different properties (e.g. stiff, soft, pointy) are hard to fabricate by quantitative parameters. Conventional 3D printing depends on slicing software, which often struggles to reproduce such fine and delicate features with the required precision, resulting in suboptimal outcomes or outright failures.

This paper proposes X-Hair, a design and fabrication workflow that allows normal users to design and create objects with kinds of hair-like structures through low-cost and accessible FDM 3D printers. To extend the manufacturing space of hair-like structures, X-Hair provides a two-step suspend printing method with controllable extruding and stringing process. By adjusting key parameters including Extrusion Length Ratio and Total Length, X-Hair achieves hair-like structures with various forms and properties based on a series of experiments. Furthermore, X-Hair utilizes Non-planar Suspend Printing to print hair-like structures on 3D models and tests optimal settings for other parameters such as temperature, extruding and stringing speed. To leverage X-Hair for novice users, we integrate our printing method and experiment results into a design tool that allows users to customize hair-like structures on diverse 3D printed models and automatically generates G-code files for 3D printing. Last, we provide various examples of hair-like structures for different functions including biomimicry, decoration, heat preservation, adhesion, and haptic interaction.

This paper presents the following contributions:

- A two-step (Extrude and String) suspend printing method based on a series of experiments to adjust Extrusion Length Ratio and Total Length that can fabricate hair-like structures with multi-property.
- An integrated software to support users to customize and fabricate 3D objects with multi-form hair and automatic G-code generation.

- Application examples based on a systematic design library showing hair-like structures with multi-function including decoration, heat preservation and interaction.

2 RELATED WORK

2.1 Personal Fabrication of Textured Objects

The use of personal fabrication technology, such as 3D printing and laser cutting, to create textured objects, is of increasing interest in the HCI community. Applying textures to 3D objects not only enhances their visual realism but also provides a richer haptic interaction experience [48]. Previous work has achieved the manufacturing of textured objects by adding them to virtual models [7], nozzle movement during printing process [25, 44], printing directly onto the surface of fabrics [23, 39]. In order to introduce more complex textural structures, researchers have combined techniques such as 4D printing [1, 9, 10, 29, 37] and 3D printing pens [32, 43], employing post-processing methods to manufacture textured objects. Aside from haptic interaction, these textures have also been applied in fastening and connecting [6, 21, 31, 38]. In addition to solid textures, PunchPrint [4] successfully added fiber textiles onto the surface of 3D-printed objects through punch needle embroidery.

Hair, as a unique form of texture, offers a more diverse visual and haptic texture palette. Researchers in personal fabrication have presented some methods to prototype objects with hair textures. Laput et al. [14] exploit the stringing phenomena of FDM 3D printers to fabricate hair-like structures. With more advanced DLP printing, Ou et al. [22] printed more delicate hair for applications as passive actuators and swipe sensors. Dyer et al. [26] built up a geometry library with collections of 3D printed textiles, textures, and hair-like structures. Utilizing hair-like structures in different fields, recent researchers enhanced the performance of texture perception in VR [3], haptic display [34], personalized figurines [5] and sensing function [12].

In comparison to prior works, X-Hair realizes more hair forms including Barb, Fluff and Curly Hair (Figure 2) through two-step suspend printing by adjusting Extrusion Length Ratio. Second, through experiments, X-Hair enables parametrical stiffness control and summarizes the parameter settings for customizing hair to make the work reproducible. Moreover, X-Hair allows printing hair on 3D models through Non-planar Suspend Printing and automatic model segmentation. X-Hair aims to explore the broad properties of hair-like textures of 3D printed objects, from rigid to soft, from straight to curly, expanding the boundaries of manufacturing spaces with embedded hair-like textures.

2.2 Advanced Manipulation with Personal Fabrication Devices

In the field of HCI, researchers are not only utilizing existing equipment and technology for personal fabrication but also seeking to expand the design space of devices through modification and advanced manipulation [11, 24]. For instance, LaserFactory [19] integrates electro-mechanical assembly and manufacturing platforms onto laser cutting machines, enabling automatic assembly of functional devices and robots. Desktop Electrospinning [27] has developed a new 3D printer that combines rigid plastic printing with

	Device	Form					Printing Strategy
		Bristle	Barb	Fluff	Fine Hair	Curly Hair	
3D Printed Hair [14]	FDM	✓			✓		Extrude and Draw
Cillia [22]	DLP	✓			✓		DLP
Extruder-Turtle [26]	FDM	✓			✓		Bridge and Wall
Desktop Electrospinning [27]	Manipulated FDM			✓			Hardware Manipulation
Enhancing Texture [3]	DLP	✓			✓		DLP
X-Hair	FDM	✓	✓	✓	✓	✓	Two-step Suspend Printing

Figure 2: Related works on 3D printing hair-like structures.

melt electrospinning to create thin fibers. Print Paths Key-framing [17] achieves non-planar layered printing by attaching a nozzle to a robotic arm.

Rather than specific modifications on the hardware, other works achieve unique printing effects at the software level with off-the-shelf 3D printers and materials, largely lowering the barrier for the masses. 3D Printed Fabric [33] simulates the weaving process by setting pre-printed pillars and controlling the printing path to manufacture Printed Fabric. Expressive Fused Deposition Modeling [35] controls Extruder Height and Extrusion Amount to print roads with different structures, creating prints with different textures. Furthermore, DefeXtiles [8] proposes under-extrusion to print woven-like textiles. To achieve more flexible control over parameters and printing paths and to overcome the limitations of existing slicing software, some works directly edit or generate G-code files. Extruder-Turtle introduces a Geometry library for directly generating G-code, enabling the manufacture of suspended structures such as fine filaments. In addition, X-Bridges and All-in-One Print [15, 30] generate bridge structures with G-code and weave them into the G-code generated by slicing software, achieving the manufacture of flexible, movable structures.

Unlike traditional layer-by-layer 3D printing, we utilize the stringing phenomenon of filament produced by *suspend printing* to create finer hair at the next level. Such stringing is often seen as a byproduct of incorrect 3D printing parameter settings and should be avoided during printing. We incorporate this stringing phenomenon as fine hair into existing models through G-code programming, integrating it into the corresponding positions of the original models, resulting in appropriate G-code files that can be used for hair printing.

2.3 Interactive Design Tools for Fabrication

Interactive design tools have been widely explored for their necessary role in digital fabrication, especially those with advanced manipulations. Some design tools provide a predefined library of shapes or structures, to help novice users understand the space for design and customization [16, 18, 45]. For instance, A-line [40] provides a library of example shapes from which users can select an example shape and further design it into more complex geometries. Other tools are based on user-input models and parameter settings,

automatically modifying the models and generating executable files to help ordinary users complete reverse design [2, 13, 36, 42, 46]. Pop-up Print [20] integrates the proposed folding method into the design tool, automatically simulating the folding of user-input models and generating folded models that can be sliced for printing. 4D Mesh [41] automatically flattens user-input surfaces and generates G-code files that can be directly printed. Freeform Fabrication of Fluidic Edible Materials [47] converts input solid models into toolpaths and generates G-code files for ink printing. Developable Metamaterials [28] transforms input solid models into ruffle structures and generates additional strips for multi-part connections.

Our design tool allows users to input their models, select the areas where they want to add hair, and customize the forms and properties of the hair. At the same time, it provides a real-time preview of the model with added hair. Ultimately, it will generate G-code files that can be directly used for printing.

3 OVERVIEW

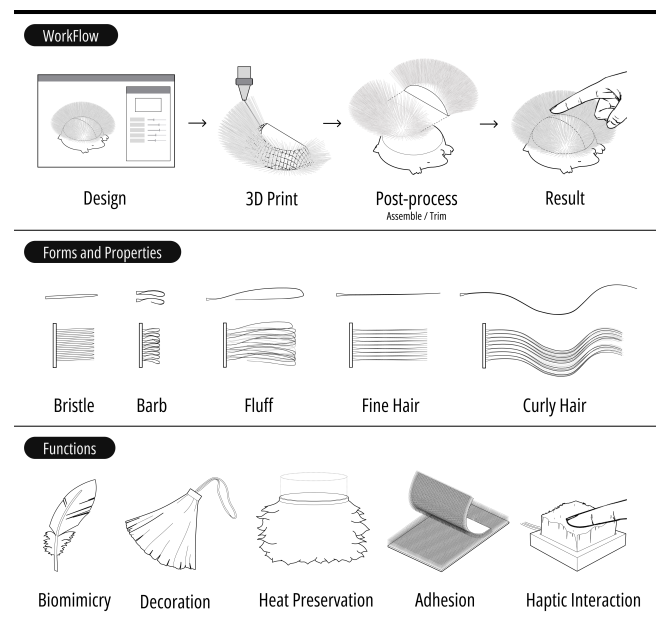


Figure 3: Overview of X-Hair.

X-Hair intends to expand the boundary of FDM 3D printing to fabricate 3D objects with multi-form hair-like structures, thus opening up new design spaces to the maker community (Figure 3). X-Hair provides software for users to design and customize hair-like structures on solid models. With a new printing method and a series of experiments, X-Hair summarizes how to fabricate hair-like structures with different forms and properties by adjusting printing parameters and integrating them into the software. Based on this, X-Hair realizes various applications and tries to take advantage of the functionality of the hair-like structures.

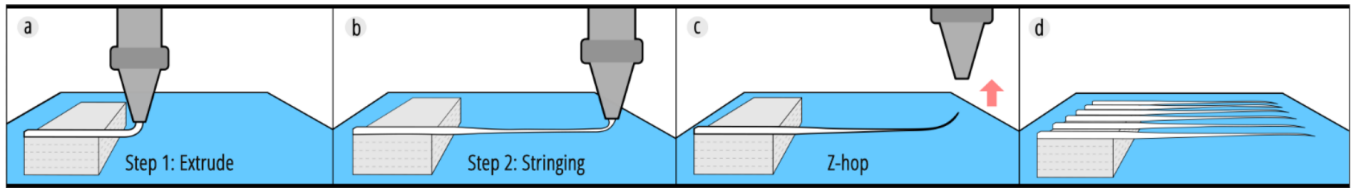


Figure 4: Two-step Suspend Printing.

4 X-HAIR METHOD

The strategy of conventional FDM 3D printing relies on two key elements: (1) a solid foundation and (2) consistent extrusion to ensure the quality of prints. By subverting these two elements, we 3D print hair of next-level fineness in mid-air from a printed foundation which supports the printing hair (Figure 5), by the method called “Two-Step Suspend Printing”. Compared to previous methods, our approach realizes the creation of strands with varying stiffness, opening up the possibility for a wider range of hair-like structures.

4.1 Two-Step Suspend Printing

To create varying fineness of a single printed strand, we invent a two-step printing strategy to consist of direct control of the printer. Step 1: the printer extrudes filament regularly. Step 2: without any further extrusion, the printer raises its moving speed to elongate the small amount of filament remaining in the nozzle into the fine strand. Technically, the printing process of one strand consists of four procedures (Figure 4):

- Extrude:** The printer moves from the start point to the switch point with regular extrusion (Step 1).
- Stringing:** The printer moves fast from the switch point to the endpoint without extrusion (Step 2).
- Z-hop:** The filament gets retracted and the printer raises in Z-axis to cut the strand and avoid redundant material (Finishing).
- Reloading:** The printer travels to the start point with little extrusion to fill the emptied nozzle, ensuring enough extrusion for the following printing. (Preparing next printing)

By inputting the coordinates of the start and end points of each hair, the Two-Step Suspend Printing method can control the printer to execute the above commands in a loop to complete the printing process. Due to the existence of the Reloading procedures, Suspend Printing can be interspersed between rigid printing without affecting the printing quality and extrusion amount of non-hair parts, which has been validated through our tests. Furthermore, by adjusting the ratio of extrusion to stringing in each hair, we can create various shapes and types of hairs with different functions, as will be demonstrated in Section 5.

4.2 Key Parameters: Extrusion Length Ratio and Total Length

X-Hair needs several parameter settings to ensure success and customize performance. Among all the parameters we tested, stringing speed, extrusion length ratio, and suspend length are dominant. Besides, we have other parameters to ensure the hair-like structures

are successfully printed, such as printing temperature, printing angle, and hair density, which we will discuss and evaluate in detail in Section 4.3.

Extrusion Length Ratio (α) & Total Length (L): As Figure 5 shows, extrusion length (l_e) and stringing length (l_s) indicate the printing length of the two steps. These two parameters regulate the stiffness of the strands and are decisive for the final form. To show the relative relationship between the two parameters and illustrate how we print different forms of hair-like structures, two more advanced parameters are applied:

$$L = l_e + l_s$$

$$\alpha = l_e/L$$

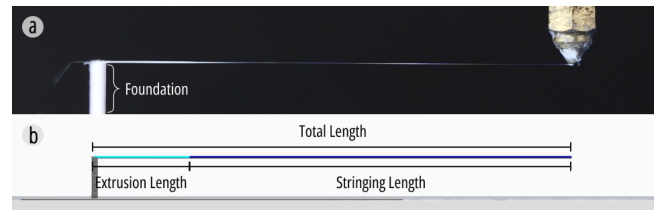


Figure 5: Schematic diagram suspend printing parameters.

Extrusion Length Ratio (α) and Total Length (L) are dominant for the properties of the printed hair-like structures. We printed a series of samples with a Total Length of 30 mm to 200 mm and an Extrusion Length Ratio from 5% to 100%. All samples are printed with a solid foundation of 20 mm in length and 10 mm in height. We use commercial PLA filaments (PolyMaker Polymax) and FDM 3D printers (Prusa MK3S+) with 0.4 mm print path and 0.2 mm layer height to fabricate the experiment samples.

First, as Figure 6 shows, α is positively correlated with the stiffness of printed hair-like structures, meaning that the stiffness gets enhanced with α increasing. And L mainly influences how easily the strand can be cut off and what the final state of the strand is. When L is short enough, the hair-like structures can be successfully printed without the additional wall (Figure 6a, b and c). Otherwise, the strands are intertwined with each other resulting in a failed test. Therefore, we make an additional wall to support the strands for these samples (Figure 6d and e).

We started without the additional wall. When $\alpha < 10\%$, the strands are extremely soft. With L increases, the strands get more fluffy. We name this form as **fluff** (Figure 6c). If α exceeds 10%, the strands cannot be cut off when stringing and the printer travels

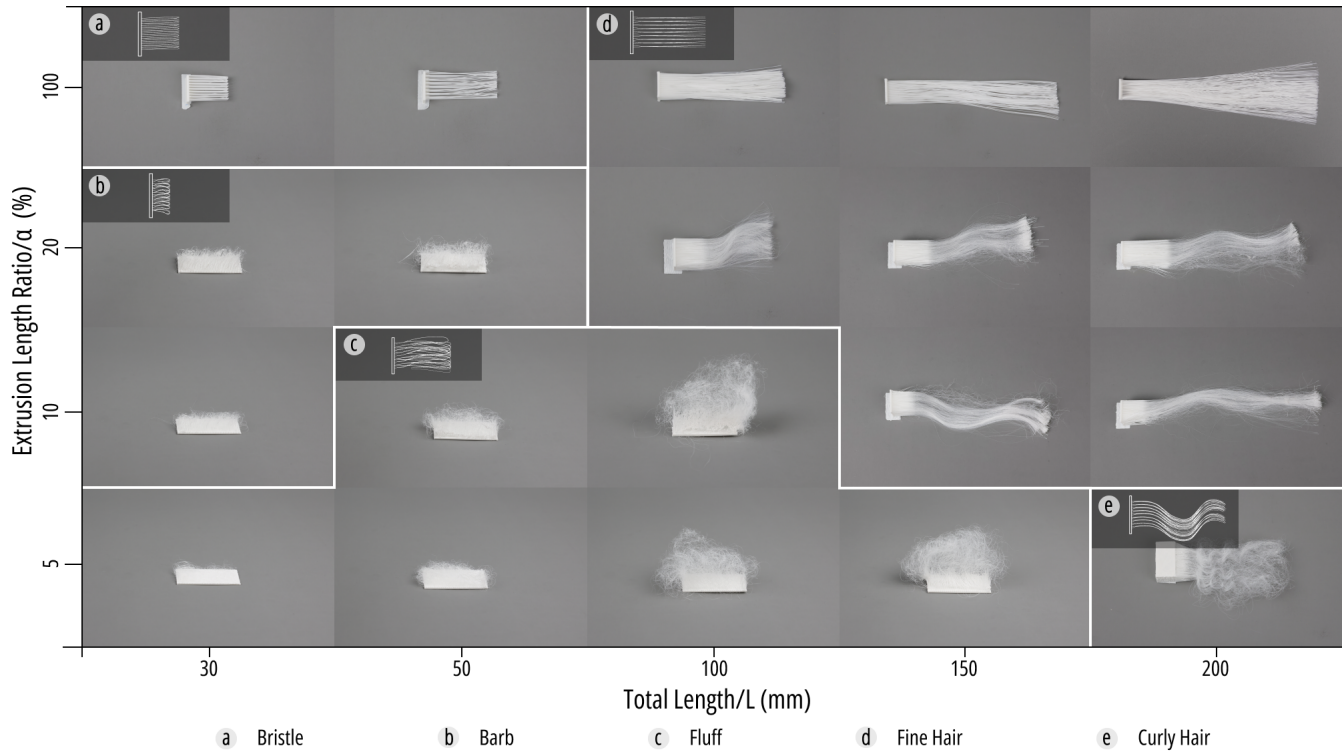


Figure 6: Printing tests with different parameters. All samples are printed at 200°C with printing angle of 0° and space between adjacent hair of 0.5mm.

back to form a little hook at the end of the strands when $L < 50$ mm. This kind of sample can be attached to the same sample tightly. Therefore, we name it **barb** (Figure 6b). We have tried to print samples with longer L and higher α excluding from Figure 6, but they all failed because of too much filament extruded or too long strand. When α increases to nearly 100%, the strings get stiff with a pointed end which we name as **bristle** (Figure 6a).

For other samples with additional walls, the strands are neater and longer. Most of them get a little curly because the strands store internal stress during fast stringing and relieve it after trimming. When $\alpha > 10\%$, the strands bend a little and we name them as **fine hair** (Figure 6d). When $\alpha < 10\%$ and $L > 200$ mm, the strands have large stress and bend a lot after trimming to form **curly hair** (Figure 6e). Furthermore, we found that α has effects on the stiffness of the strands. As Figure 7 shows, we display four samples of total length 50 mm as examples. With α increasing, the strands gets subtler and subtler when touched. When $\alpha > 40\%$, the variation becomes quite tiny and hard to observe and feel.

4.3 Other Parameters and Optimizations

Printing Temperature: In the printing process, the nozzle temperature is a critical parameter in 3D printing settings and plays a significant role in determining the success rate of fabricating hair-like structures. Among the types of hair that we can print, the fluff presents the highest difficulty in fabrication. Consequently, we

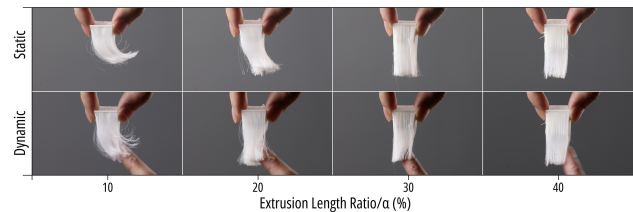


Figure 7: Printing tests with different extrusion length ratios ($L = 50$ mm).

conducted tests to determine the temperature range that promises more fluffy strands can successfully be formed, which we have now integrated as our overall temperature setting for all our hairy forms.

As PolyMax PLA has a recommended nozzle temperature range of 190°C to 230°C, we established five test points and performed printing tests with a total length of 100 mm at an ambient temperature of 20°C. The optimal temperature range for printing fluff is found to be between 190°C and 210°C (Figure 8). Within this range, the extrusion success rate was highest, and the printed fluff exhibited the most desirable fluffy appearance. Therefore, the recommended temperature range for printing fluff is 190°C to 210°C.

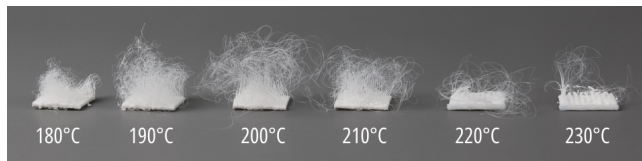


Figure 8: Samples of different printing temperatures.

Non-planar Suspend Printing: In addition to printing hair-like structures horizontally, we can further Non-planar Suspend Printing in other directions. We define the printing angle as the angle between the hair direction and the printing platform, with a maximum range of -90° to 90° . We tested the angle range of Non-planar Suspend Printing from -90° to 90° . We used the same material and set the printing temperature to 200°C to print multiple Bristles at different angles within the same layer.

We found that starting from different points, Non-planar Suspend Printing allows for a comprehensive printing angle range from -15° to 90° (Figure 9a and b). However, starting from the same point, Non-planar Suspend Printing is limited to -15° to 45° (Figure 9c and d). This limitation is due to the over-approaching of the heated print head, which can cause softening of the roots of already printed hair, thus affecting quality.

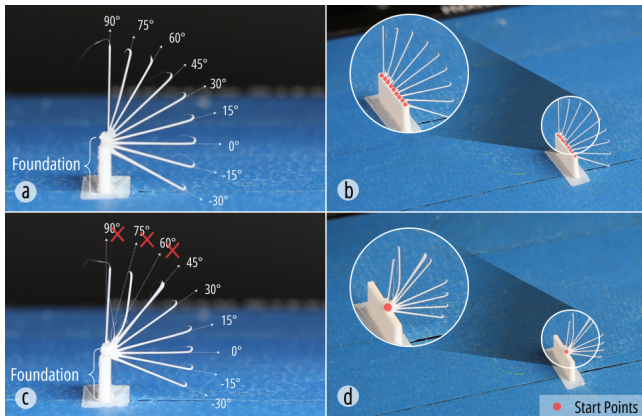


Figure 9: Non-planar printing of angles from -30° to 90° : (a, b) Starting from different points; (c, d) Starting from the same point.

Hair Density: Hair printing density is also a crucial factor influencing its texture. We further control the printing path details to address this issue. Printing high-density hair presents two main challenges: Challenge 1: Collision between the heated nozzle and existing hair during printing leads to damage; Challenge 2: Hair strands being too close together causing them to stick to each other. To address the challenges and realize high-density hair printing, we further optimize printing control by starting extruding inside the foundation and setting the default print angle of 3° . Starting extruding inside the foundation makes the strands not easy to stick. Setting the default print angle of 3° makes the nozzle away from the printed hair.

Using the above methods, we challenged and tested high-density hair printing, ultimately achieving the manufacturing of fine or curly hair with a minimum space between adjacent hair of 0.2 mm , as shown in Figure 10.

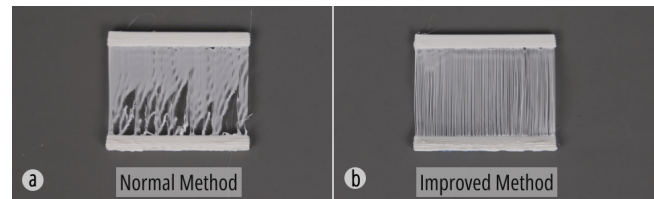


Figure 10: Printing test of 0.2mm space between adjacent hair: (a) Normal Method; (b) Improved Method.

Extrusion Rate & Extrusion Speed: Based on our tests, we found that extrusion rates ranging from 25% to 200% all produced effective results with little difference in strand diameter. Therefore, we typically set the extrusion rate at 100%. Similarly, we tested extrusion speeds from 500 mm/min to 5000 mm/min and found that the speed was not critical for the printing qualities. Instead, the stringing speed had a more significant impact. To ensure successful prints, we set the extrusion speed at 1000 mm/min .

Stringing Speed: Stringing speed refers to the speed of the nozzle without actual extrusion, but elongating the remained filament within the nozzle. Stringing speed has a critical impact on the effect of the final strands. Without enough stringing speed, the strand will not be fine enough, which further leads to sagging due to gravity, affecting the overall qualities of the hair-like structure. When the speed is too fast, the strand will be instantly cut off, causing direct failure of the printing. It has been validated in our test that a stringing speed of 7000 mm/min to 9000 mm/min is the most suitable range for fine hair printing. We set a stringing speed of 8000 mm/min as a default parameter for most cases of our printing.

4.4 Post-processing

X-Hair needs two kinds of post-processing methods:

Assemble: For complex models that cannot be fabricated in a single print run, our approach involves segmenting the model into multiple parts for individual printing (See details in Section 6.2). After printing, all the printed parts are then assembled to achieve the fabrication of the entire model.

Trim: In the cases that the user wants to produce neatly aligned hair-like structures including fine hair and curly hair, it is necessary to print an additional wall for support (Figure 11a), so that the filaments can adhere to the wall to form a neat arrangement. After printing, the wall is then cut with a tool such as scissors to create neatly aligned hair-like structures like fine hair (Figure 11b and c).

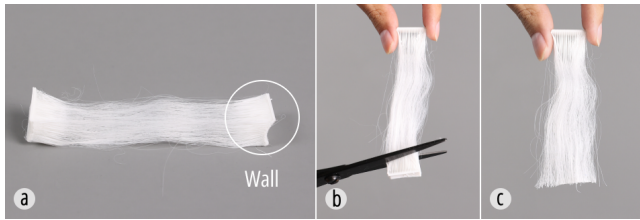


Figure 11: The process of trimming: (a) A printed sample with $\alpha = 10\%$ and $L = 100$ mm; (b, c) Cut the wall off with scissors to form fine hair.

5 DESIGN LIBRARY OF X-HAIR

Based on the various parameter controls outlined in the previous chapter, we have developed a structure library for the biomimetic printing of various forms of hair found in nature (Figure 12). This library encompasses a spectrum from rigid to soft, straight to curved, and from stiff to fluffy. Based on their different forms and properties, we classify them into five categories: bristle, barb, fluff, fine hair, and curly hair.

5.1 Bristle

Bristle is typically stiff and erect, referring to the coarse hairs found on animals such as pigs and horses. In everyday tools, bristle is commonly used in brushes, cleaning tools, and paintbrushes. Its diameter, usually over 0.2 millimeters, and uniform structures make it relatively easy to manufacture in 3D printing. In suspended printing, controlling α at 100% means the hair is extruded normally. This results in a symmetrical, rigid filament structure for bristle.

Additionally, X-hair is capable of increasing the extrusion amount, achieving a maximum diameter of 0.6 mm for bristle, further enhancing its hardness. The density of bristle can also be adjusted to suit different functionalities, such as water absorption and cleaning ability. By adjusting α to 80%, the bristle tips become softer, suitable for cleaning delicate objects like skin or jewelry.

5.2 Barb

Feathers are essential growths for bird flight. Barbs are the main components of a feather, connected to a central axis called a vane, collectively forming the shape and function of the feather.

Through precise control in suspend printing, we can achieve biomimetic manufacturing of barbs in off-the-shelf FDM 3D printers. In the feathers printed with X-hair, we first print a hollow central shaft and then perform suspend printing on it. In detail, in the manufacturing of each 50 mm barb, we extrude for the first 15% and then perform stringing for the remaining 85%. This composition ratio ensures both the minimum diameter at the tip of the barb, together with the straightness.

5.3 Fluff

Fluff, unlike the first two forms of hair, exhibits a pronounced curl, with a texture closer to cotton or cashmere. Due to its smaller diameter and tangled form, it has a weaker fibrous characteristic while providing better insulation.

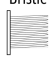

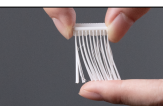
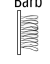











Name	Specification	Static	Dynamic
 Bristle	α : 100% L: 1–100mm Interval: 1.0mm Wall: No		
 Barb	α : 10%–20% L: 30–50mm Interval: 0.6mm Wall: No		
 Fluff	α : 5%–10% L: 50–150mm Interval: 0.6mm Wall: No		
 Fine Hair	α : 10%–40% L: 30–300mm Interval: 0.4mm Wall: Yes		
 Curly Hair	α : 3–5% L: 200mm Interval: 0.4mm Wall: Yes		

Figure 12: Design Library of X-Hair.

To achieve its effective curl, we modify the suspend printing where, instead of using Z-hop, we control the nozzle to suddenly hop in a direction away from the root of the hair, while retracting the printing material. This action causes the hair to break suddenly and rebound. Since the hair has just been printed, it is in a heated state and will rapidly cool to room temperature after rebounding, finally retaining its curled state. The randomness of this rebound angle also naturally presents its shape in a spherical form.

5.4 Fine Hair & Curly Hair

When 3D printing hair longer than 100 mm, suspend printing faces a significant challenge of drooping, which can lead to hair strands sticking together. To address this, we add a support wall to better secure both ends and prevent sticking. We then remove the support wall on the other side through post-processing, achieving long and fine hair structures. By controlling different α values, the hair will exhibit different textures. A larger α will increase the weight of the hair, giving it more sag; a smaller ratio will make the hair finer and lighter, creating a curly effect.

6 SOFTWARE

To help users better understand X-Hair workflow and provide customized design, we implemented software using Rhinoceros¹, Grasshopper² (a visual programming plug-in for Rhinoceros), and Human UI³ (a plug-in for Grasshopper). Users can import their models into the software and select certain surfaces to attach the hair-like structures. The software allows users to customize their desired structures by choosing hair forms and adjusting parameters.

¹<https://www.rhino3d.com/>

²<https://www.grasshopper3d.com/>

³<https://www.food4rhino.com/en/app/human-ui>

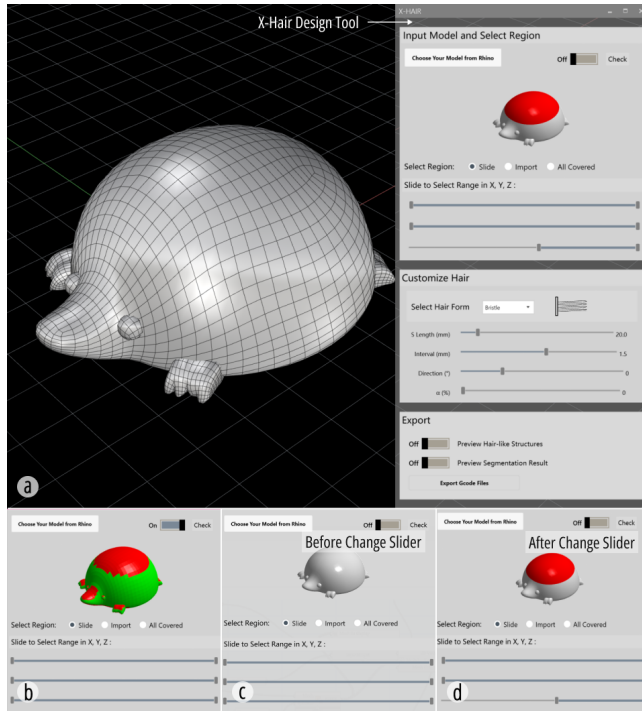


Figure 13: User Interface of X-Hair: (a) Importing a hedgehog model; (b) Checking the printability of each surface; (c) Before selecting regions to attach hair-like structures; (d) Sliding to select regions.

Finally, files will be generated automatically, which are ready for 3D printing directly.

6.1 Design Goals

X-Hair software is designed with a few goals:

- The interface should be user-friendly enough with standard steps in adjustment.
- The software should provide users with highly customized design options for hair-like structures including forms, length, density, etc.
- The software is able to add hair-like structures on the input model and generate the files ready to print automatically.

6.2 User Workflow

Import and Select: As a customized design software, the work begins with the user importing a 3D model from Rhinoceros. To ensure the final model can be 3D printed while maintaining an acceptable computing efficiency, the tool simplifies the imported model using a low-poly operation. Before selecting regions to attach hair-like structures, users can check the printability of each surface. Regarding the results from the printing angle experiments, the surfaces suitable for printing are marked as green. Otherwise, the surface will be marked as red for warning. Based on this, users can select regions on the model to attach hair-like structures. The software provides three options to select regions, including sliding (Figure

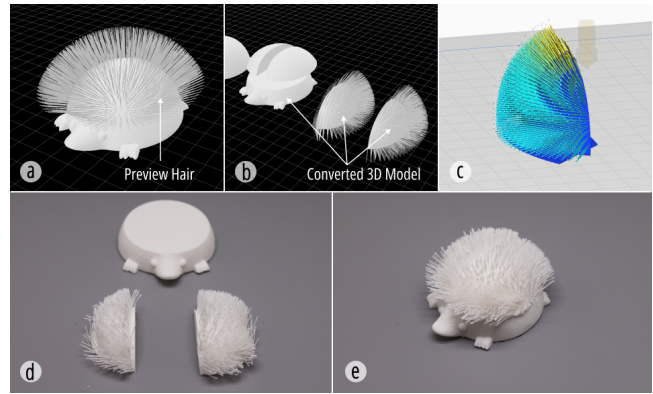


Figure 14: Preview and Exporting files of a hedgehog: (a) Preview the whole hedgehog model with bristles; (b) Preview the segmentation results; (c) Preview the G-code files in slicing software; (d) The printing results of each separated part; (e) The final result after assembling.

13c and d), importing a surface from Rhinoceros, or covering all surfaces of the model. If the selected region encompasses elements that are unprintable, our software is designed to subsequently segment the model into multiple printable parts, each of which will have its corresponding G-code files generated independently.

Customize Hair-like Structures: Our software allows users to customize their desired hair-like structures by choosing hair form and adjusting corresponding parameters. First, users choose one from five given hair forms. Then users set parameters including Extrusion Length Ratio, Total Length, Interval, and Direction. To help users set these parameters in the proper range, our software will automatically change the upper limit and lower limit of each slider according to the chosen hair form.

Preview and Export: In the design process, our software allows users to preview the results of the model with hair-like structures (Figure 14a). The hair-like structures will change in real-time if users modify the parameters. For the model that needs to be segmented, our software provides a preview of the segmentation results for users to check (Figure 14b). Last, users can export all the files to print (Figure 14c).

6.3 Computational Pipeline

Input Analysis: In the initial phase, our software analyzes the imported model to adequately prepare it for subsequent procedures. To this end, we first transform the imported model into a quad mesh and then reduce the mesh density to facilitate computational efficiency. However, due to the limitation within Rhinoceros that prevents individual mesh faces from being previewed or selected, it is necessary to convert all mesh faces into surfaces to enable their marking and selection. This conversion process entails deconstructing each mesh face into its constituent four vertex indices. Following this, we further deconstruct the mesh to isolate vertices, subsequently locating their corresponding counterparts based on

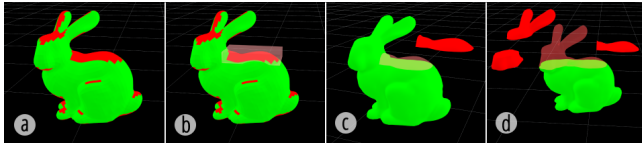


Figure 15: The Segmentation Pipeline: (a) Calculate the normal vector of each mesh and label them in green(printable) or red(unprintable); (b) For each red part, generate its bounding box and obtain the intersection shape of the box and the whole model; (c) Separate the intersection part from the model; (d) Repeat (b)-(c) until all the separated parts are printable.

these indices. Through this method, we can connect the four vertices, thereby constructing a surface. After that, the surfaces will be checked and marked as green or red in the interface.

Segmentation: Due to the limitation of the printing angle, the hairy entity in some cases cannot be 3D printed as a single part. As shown in Figure 15, if users want to print hair-like structures along the normal vector on the whole Stanford Bunny, obviously the direction of the hair on the bunny’s back, and head exceeds the suitable range. Therefore, we need to segment the bunny into several parts. First, we calculate the normal vector of each mesh to check if it can be printed according to our experiments. For each unprintable part (marked as red in Figure 15), if its area is smaller than 1 cm^2 , it will be neglected. Otherwise, the software generates the bounding box of the part and calculates the intersection shape of the box and the bunny model. The intersection part will be separated from the model. We chose the bounding box to do the segmentation because it can promise that at least one surface of the separated part is flat so that it can be attached to the printing platform. Finally, the software gets all separated parts and rotates them to ensure they are printable.

G-code Generation: As the essential and final step in our procedures, the software automatically generates files for 3D printing. To achieve this, we separate a model into two parts: the solid model and the hair-like structures. First, we slice the solid model into layers of outline through the Contour command in Grasshopper. For each layer, we offset the outline several times to make the outer wall. We create a 3D mesh to do Boolean operations with the solid model to get the infill structures. The outer walls and infill structures will be divided into points to generate instructions. Second, we abstract the hair-like structures into lines. For each line, we can easily obtain its start point and end point. As each line is printed by our two-step suspend printing method, we apply the Evaluate Curve command to extract the point to divide the line into two parts. Finally, our software transfers all the points into G-code instructions in order using a Python script.

7 APPLICATIONS

Our software enables 3D printing users to incorporate hair-like structures onto target objects. Consequently, users can emulate hair-like structures found in nature or customize common fur-based products from everyday life. Additionally, this capability enables the

exploration of novel haptic interfaces with unprecedented haptic experiences.

7.1 Emulating Hair Forms in Nature

Both animals and plants in nature exhibit distinctive hair-like structures. Our software enables the emulation of numerous intriguing structures while providing users with the space of personalizing. For certain intricate structures that cannot be directly 3D printed as a single piece, we will employ a modular assembly approach.

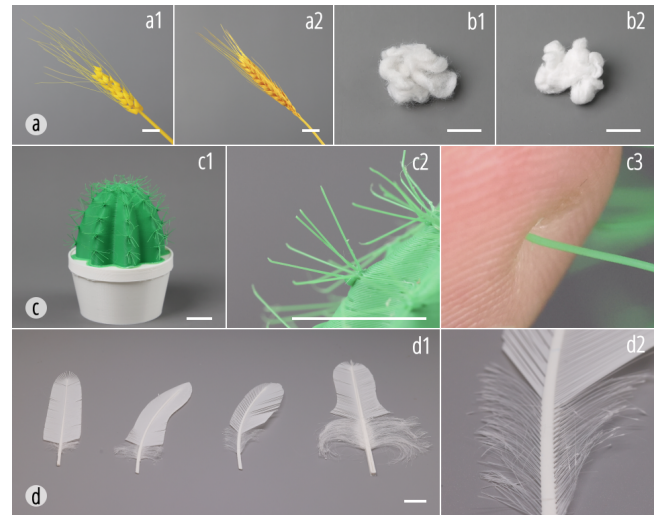


Figure 16: Examples X-hair can create: (a) 3D printed wheat (a1) vs. real wheat (a2). (b) 3D printed cotton (b1) vs. real cotton (b2). (c) A printed cactus with bristles; (d) X-Hair Feathers with various shapes. Scale Bar: 20 mm.

Wheat and Cotton: The spikelets of wheat possess slender, needle-like projections known as awns. Our software enables the precise printing of individual spikelets with awns, facilitating the assembly of realistic wheat spike models (Figure 16a). Similarly, our software can also produce cotton using curly hair (Figure 16b).

Cactus: The surfaces of cactus exhibit bristles and characteristic of them is the presence of multiple rigid filaments protruding at various angles from a central point of origin. Users can leverage our software to incorporate and print such hair-like structures onto desired surfaces, as seen in Figure 16c.

Feather: Bird feathers are also a type of hair-like structure, exhibiting two different characteristics on the same feather: the tip is composed of stiff barbs, while the base consists of soft afterfeathers. Through the arrangement of scale-like structures, they acquire unique properties such as wind and water resistance externally, and insulation internally. Using 3D printing control of X-hair, we can manufacture two completely different types of feathers on the same shaft. (Figure 16d).

Dandelion: The fruiting bodies of dandelions exhibit a long, filamentous structure. Consequently, users can employ our software to print the intricate filaments found on dandelion seeds. Although

we cannot print an entire dandelion flower in a single print, we can individually print each component and assemble them onto a central head, thereby recreating the overall inflorescence morphology. As seen in Figure 17, we printed 50 dandelion seeds and assembled them into a whole dandelion. This modular approach allows for the faithful replication of complex natural structures that would otherwise be challenging to fabricate as a monolithic entity.

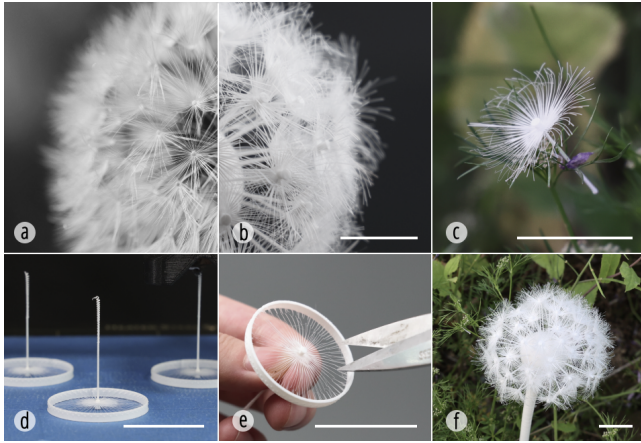


Figure 17: (a) Real dandelion; (b) A 3D printed dandelion; (c) A 3D-printed seed of dandelion; (d) Printing the seeds of dandelions; (e) Trimming the supporting wall; (f) A 3D printed dandelion on the grass. Scale Bar: 20 mm.

Stanford Bunny: The overall shape of a rabbit is considerably intricate, exhibiting a soft, downy texture across its entire body. In the previous section showcasing software operations, we demonstrated printing fluff only on the rabbit’s back. However, our software can readily extend this approach to print fluff across the entire rabbit model using the same methodology. Our software segments the rabbit model into constituent parts and adds fluff to the corresponding regions on each part, and the user then manually assembles these components to form the complete rabbit figure (Figure 18).

7.2 Customized products with Hair

Hairy Products are pervasive in our daily lives. Our software offers a streamlined approach to customizing and fabricating such products according to individual preferences and requirements. This empowers users to create personalized versions of familiar hairy items, enabling greater creative expression.

Wig: Wigs offer individuals an opportunity to experiment with diverse hairstyles and colors without committing to any alteration of their natural hair. Leveraging our software, we have fabricated a wig patch with a fixed structure. Users can create personalized wig segments featuring a wide range of hair-like structures (Figure 19). This approach empowers individualized self-expression through the customization of wig patches, allowing users to craft unique and distinctive hairstyles that reflect their personal aesthetic preferences.

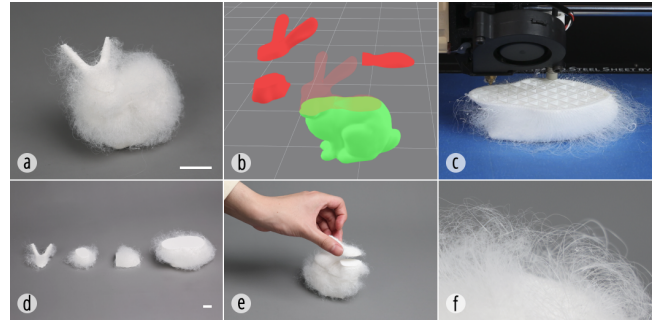


Figure 18: (a) A 3D-printed Stanford Bunny with fluffy hair; (b) Separated parts of the bunny in X-Hair software; (c) Printing process of one part; (d) Printing results of separated parts; (e) Assembling the rabbit; (f) The detail of the fluff on the rabbit. Scale Bar: 20 mm.

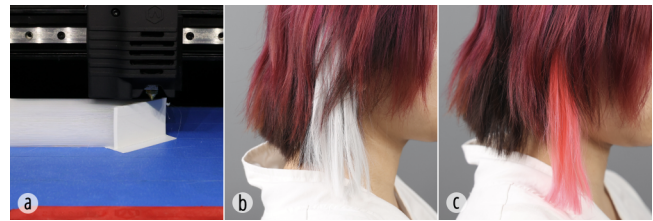


Figure 19: Customized wigs: (a) Printing process of a wig; (b) A white wig; (c) A red wig.

Shuttlecocks: We can also customize various feather-based artifacts. As an illustrative example, we consider feather shuttlecocks. Within our software, users can design and tailor the size and shape of the feathers. The color also can be changed by different PLA materials (Figure 20). This level of customization allows for the creation of unique feather shuttlecock designs that deviate from traditional configurations, enabling users to explore novel scenarios. In practical use, regular shuttlecocks 3D printed with the X-hair method perform very similarly to commercial shuttlecocks, exhibiting nearly identical movement trajectories and impact sensations.

Brush: Our software enables the customization of brushes with varying bristle stiffness and distribution patterns. By assigning different hair-like structures to distinct regions within the software, or selectively omitting hair deposition in certain areas, we can create a diverse range of brush textures (Figure 21). After a simple trimming process, these custom-printed brushes can be directly employed for artistic expression.

Hairy Lamp: Designers and artists can also utilize our software to design lighting fixtures with hair. The internal light can shine through the hair, creating a beautiful gradient of light (Figure 22).

7.3 Hair for Interaction

By leveraging our software’s ability to fabricate hair-like structures, we can introduce new decoration, haptic experience, and sensory function to tangible interfaces. This approach enriches the user

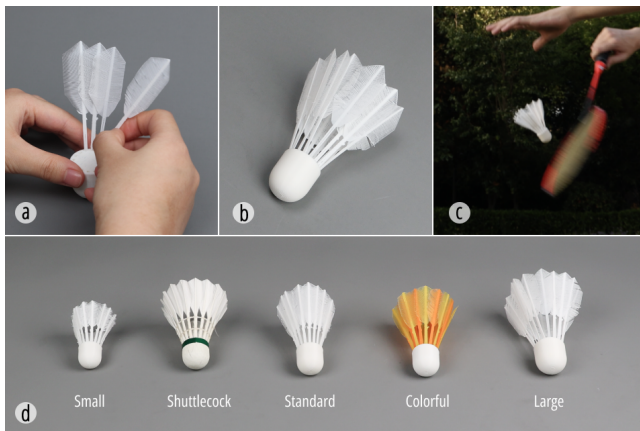


Figure 20: (a) Assembling a 3D printed feather shuttlecock; (b) A standard 3D printed feather shuttlecock; (c) Hitting the shuttlecock with a racket; (d) Customizing 3D printed feather shuttlecocks with different sizes and colors.



Figure 21: 3D Printed Brushes: (a-c) Brushes with varying stiffness; (d) Writing with a 3D printed brush. Scale Bar: 20 mm.



Figure 22: Hairy Lamp. Scale Bar: 20 mm.

experience and opens up new avenues for intriguing and intuitive interaction with devices.

Cup Sleeve: Certain animal furs possess insulating properties, enabling effective heat retention. For instance, the fur of polar bears exhibits excellent thermal insulation capabilities. In essence, these thermally protective furs derive their insulating properties from their intricate microscopic structures. Interestingly, we have discovered that the 3D-printed hair-like structures fabricated using

our method also exhibit notable insulating properties. Leveraging this finding, we have created an insulating cup sleeve that can prevent users from experiencing discomfort or burns when handling hot beverages (Figure 23).

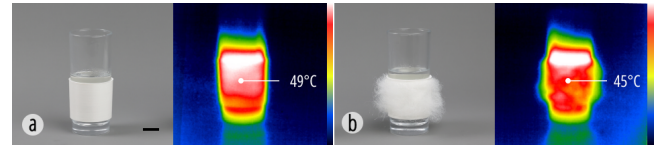


Figure 23: Cup Sleeve printed with X-hair method: (a) A cup sleeve without hair; (b) A cup sleeve with fluff. Scale Bar: 20 mm.

Velcro Ball: Hook-and-loop fasteners, commonly known as velcro, feature protruding hook-like structures that enable adhesion between complementary surfaces. Our software facilitates the customization and fabrication of such hook-like structures directly onto object surfaces, allowing for the creation of adhesive interfaces. We have fabricated a spherical velcro ball with a diameter of 60mm, featuring an array of hook-like structures on its surface (Figure 24). This ball is designed to adhere to complementary loop surfaces, enabling it to be attached and detached reversibly.



Figure 24: A 3D-printed velcro ball: (a) Throwing the velcro ball; (b) Catch the ball with velcro; (c) The detail of the ball. Scale Bar: 20 mm.

Directional hair sensor: We further exploited the piezoelectric sensors, endowing hair-like structures with directional haptic perception capabilities. To demonstrate that, we constructed a panel with fine hair and attached the end of the piezoelectric sensor to the bottom of the panel. As a finger slides over the hair, the stress induced by the bending hair slightly moves the panel, causing minor deformation to the bottom-placed piezoelectric sensor. This results in the generation of electrical signals, which vary significantly with the direction of the finger's movement.

Utilizing this principle, a controller mediated by hair-like structures can be fabricated, capable of controlling functions such as moving a character in computer games (Figure 25a) or scrolling web pages (Figure 25b) on a computer.

The hair sensors expand the hardware foundation of multi-modal tactile perception, giving freedom of interaction methods in the design space, which can enhance the user's perception and immersive participation[48].

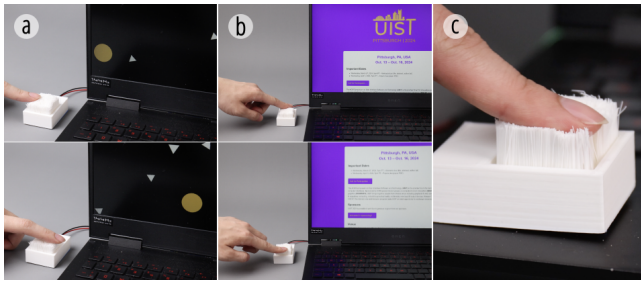


Figure 25: Directional Hair Sensor: (a) Controlling a ball in a game; (b) Scrolling web pages; (c) Touching the surface of the hair sensor.

8 DISCUSSION, LIMITATIONS, AND FUTURE WORK

8.1 Printing Quality

X-Hair focuses on the FDM 3D printing of hair-like structures and intends to improve their quality. However, these mid-air strings sometimes may affect the print quality of other parts. Firstly, the roots of the hair-like structures are attached to the solid foundation, preventing printing material from fully adhering to the previous layer, which may reduce the quality of the solid's surface. Secondly, when printing fine or curly hair, the fast stringing speed means that the strings inside store more stress. As a result, significant tensions exist at both ends of the strings, which can easily cause deformation of the solid foundations on both sides, thereby affecting the final result.

In addition, we currently generate files based on our software, which does not do as well as the slicing software in controlling details like acceleration. In the future, we will continue to explore the factors of printing hair-like structures on solids to find targeted solutions and improve the overall print quality.

8.2 Printing Time

Plenty of hair-like structures cause a substantial increase in printing time. For instance, the printing of a hairy bunny took over 10 hours, whereas printing a smooth bunny without any hair-like structures would typically require only 5h 51min (under the same conditions of no supports, a speed of 50 mm/s, a layer height of 0.2 mm, and a 10% infill ratio). The underlying reason for this disparity is evident: when printing objects with hair-like structures on the surface, a considerable amount of time is required to meticulously construct the intricate hair-like structures. Furthermore, certain forms of hair may necessitate the incorporation of additional support walls. Despite these challenges, we anticipate that future advancements in optimizing the printing path can minimize printing time as much as possible, thereby enhancing overall printing efficiency.

8.3 Bionics

X-Hair tried to emulate hair forms on various plants in nature, while the printed hair-like structures do not behave the same as real hair-like structures in waterproofing, seeding, protection and so on. To fabricate hair-like structures for bionics, we are going to

do more research on the micro structures or the material characteristics of hair-like structures in nature to understand how they work. Furthermore, we may need to try some other fabricating methods or combine 3D printing with other techniques to realize the bionic functions of hair-like structures. In summary, our ongoing exploration in the fabrication of hair-like structures aims to advance the field of bionics, with a vision of unlocking their potential applications across various scenarios including agriculture, health care, and wearables.

8.4 Electronic Hair

X-Hair aims to expand the functionality of 3D printed hair-like structures, but the use of entirely non-conductive PLA limits the capabilities of the hair-like structures. To be more exact, X-Hair uses hair-like structures as tactile or structural mediums that indirectly influence external sensors for interactive functions, but it does not fully leverage the unique properties of the hair-like structures. Regarding this, we attempted to use conductive PLA to print electrically conductive hair-like structures, which successfully resulted in hair-like structures similar to those in X-Hair. Based on that, we hope to explore the use of conductive PLA to print hair-like structures in future work and to experiment with other methods to enhance conductivity. We would also test relevant parameters and incorporate more properties such as sensing and interactive output into these hair-like structures. Furthermore, utilizing various combinations of hair forms and properties in functional components can be applied in rapid circuit fabrication. This approach allows the incorporation of hair texture and interaction characteristics into the HCI community. By integrating these unique features, the potential for creating more immersive and tactile interfaces is significantly enhanced. The ability to customize and rapidly prototype these hair-like structures will open new avenues for personal fabrication and innovative applications in human-computer interaction.

9 CONCLUSION

In conclusion, this paper introduces X-Hair, a design and fabrication workflow enabling ordinary users to design and produce objects with hair-like structures using affordable FDM 3D printers. The two-step printing method presented in this work expands the manufacturing capabilities of hair-like structures, achieved through manual crafting of instructions and a series of experiments to quantitatively realize hair-like structures with varying properties by adjusting specific parameters. To make X-Hair accessible to novice users, we have integrated our printing method and experimental findings into a design tool, enabling users to customize hair-like structures on a range of 3D printed models and automatically generate files for 3D printing. Finally, we showcase various examples of hair-like structures serving different functions, including biomimicry, decoration, heat preservation, adhesion, and haptic interaction.

ACKNOWLEDGMENTS

This project was supported by Zhejiang Provincial Natural Science Foundation of China under Grant No. LR24F020001.

The authors would also like to thank all the reviewers for their useful comments. We would also like to thank Yinan Zhang for her contribution to the revision and Kuangqi Zhu for his valuable

insights. Additionally, we would like to thank Yanghonghui Chen, Jian Wang, Zhishuai Hu for their collective participation in the early period of this project.

REFERENCES

- [1] Byoungkwon An, Ye Tao, Jianzhe Gu, Tingyu Cheng, Xiang 'Anthony' Chen, Xiaoxiao Zhang, Wei Zhao, Youngwook Do, Shigeo Takahashi, Hsiang-Yun Wu, Teng Zhang, and Lining Yao. 2018. Thermorph: Democratizing 4D Printing of Self-Folding Materials and Interfaces. In *Proceedings of the 2018 CHI Conference on Human Factors in Computing Systems (CHI '18)*. Association for Computing Machinery, New York, NY, USA, 1–12. <https://doi.org/10.1145/3173574.3173834>
- [2] Xiang 'Anthony' Chen, Jeeun Kim, Jennifer Mankoff, Tovi Grossman, Stelian Coros, and Scott E. Hudson. 2016. Reprise: A Design Tool for Specifying, Generating, and Customizing 3D Printable Adaptations on Everyday Objects. In *Proceedings of the 29th Annual Symposium on User Interface Software and Technology (UIST '16)*. Association for Computing Machinery, New York, NY, USA, 29–39. <https://doi.org/10.1145/2984511.2984512>
- [3] Donald Degraen, André Zenner, and Antonio Krüger. 2019. Enhancing Texture Perception in Virtual Reality Using 3D-Printed Hair Structures. In *Proceedings of the 2019 CHI Conference on Human Factors in Computing Systems*. ACM, Glasgow Scotland UK, 1–12. <https://doi.org/10.1145/3290605.3300479>
- [4] Ashley Del Valle, Mert Toka, Alejandro Aponte, and Jennifer Jacobs. 2023. Punch-Print: Creating Composite Fiber-Filament Craft Artifacts by Integrating Punch Needle Embroidery and 3D Printing. In *Proceedings of the 2023 CHI Conference on Human Factors in Computing Systems*. ACM, Hamburg Germany, 1–15. <https://doi.org/10.1145/3544548.3581298>
- [5] Jose I. Echevarria, Derek Bradley, Diego Gutierrez, and Thabo Beeler. 2014. Capturing and stylizing hair for 3D fabrication. *ACM Transactions on Graphics* 33, 4 (July 2014), 125:1–125:11. <https://doi.org/10.1145/2601097.2601133>
- [6] eried. 2011. *Printable Velcro*. Printables. <https://www.printables.com/model/33302-printable-velcro>
- [7] Faraz Faruqi, Ahmed Katary, Tarik Hasic, Amira Abdel-Rahman, Nayeemur Rahman, Leandra Tejedor, Mackenzie Leake, Megan Hofmann, and Stefanie Mueller. 2023. Style2Fab: Functionality-Aware Segmentation for Fabricating Personalized 3D Models with Generative AI. In *Proceedings of the 36th Annual ACM Symposium on User Interface Software and Technology*. ACM, San Francisco CA USA, 1–13. <https://doi.org/10.1145/3586183.3606723>
- [8] Jack Forman, Mustafa Doga Dogan, Hamilton Forsythe, and Hiroshi Ishii. 2020. DefeXtiles: 3D Printing Quasi-Woven Fabric via Under-Extrusion. In *Proceedings of the 33rd Annual ACM Symposium on User Interface Software and Technology (UIST '20)*. Association for Computing Machinery, New York, NY, USA, 1222–1233. <https://doi.org/10.1145/3379337.3415876>
- [9] Jianzhe Gu, David E. Breen, Jenny Hu, Lifeng Zhu, Ye Tao, Tyson Van de Zande, Guanyun Wang, Yongjie Jessica Zhang, and Lining Yao. 2019. Geodesy: Self-rising 2.5D Tiles by Printing along 2D Geodesic Closed Path. In *Proceedings of the 2019 CHI Conference on Human Factors in Computing Systems (CHI '19)*. Association for Computing Machinery, New York, NY, USA, 1–10. <https://doi.org/10.1145/3290605.3300267>
- [10] Jianzhe Gu, Vidya Narayanan, Guanyun Wang, Danli Luo, Harshika Jain, Kexin Lu, Fang Qin, Sijia Wang, James McCann, and Lining Yao. 2020. Inverse Design Tool for Asymmetrical Self-Rising Surfaces with Color Texture. In *Proceedings of the 5th Annual ACM Symposium on Computational Fabrication (SCF '20)*. Association for Computing Machinery, New York, NY, USA, 1–12. <https://doi.org/10.1145/3424630.3425420>
- [11] Scott E. Hudson. 2014. Printing teddy bears: a technique for 3D printing of soft interactive objects. In *Proceedings of the SIGCHI Conference on Human Factors in Computing Systems (CHI '14)*. Association for Computing Machinery, New York, NY, USA, 459–468. <https://doi.org/10.1145/2556288.2557338>
- [12] Kosei Kamata, Haruki Takahashi, and Koji Tsukada. 2023. Conductive, Ferromagnetic and Bendable 3D Printed Hair for Designing Interactive Objects: Conductive, Ferromagnetic and Bendable 3D Printed Hair. In *Adjunct Proceedings of the 36th Annual ACM Symposium on User Interface Software and Technology (UIST '23 Adjunct)*. Association for Computing Machinery, New York, NY, USA, 1–3. <https://doi.org/10.1145/3586182.3615823>
- [13] Jeeun Kim, Qingnan Zhou, Amanda Ghassaei, and Xiang 'Anthony' Chen. 2021. OmniSoft: A Design Tool for Soft Objects by Example. In *Proceedings of the Fifteenth International Conference on Tangible, Embedded, and Embodied Interaction (TEI '21)*. Association for Computing Machinery, New York, NY, USA, 1–13. <https://doi.org/10.1145/3430524.3440634>
- [14] Gierad Laput, Xiang 'Anthony' Chen, and Chris Harrison. 2015. 3D Printed Hair: Fused Deposition Modeling of Soft Strands, Fibers, and Bristles. In *Proceedings of the 28th Annual ACM Symposium on User Interface Software & Technology*. ACM, Charlotte NC USA, 593–597. <https://doi.org/10.1145/2807442.2807484>
- [15] Jiaji Li, Mingming Li, Junzhe Ji, Deying Pan, Yitao Fan, Kuangqi Zhu, Yue Yang, Zihan Yan, Lingyun Sun, Ye Tao, and Guanyun Wang. 2023. All-in-One Print: Designing and 3D Printing Dynamic Objects Using Kinematic Mechanism Without Assembly. In *Proceedings of the 2023 CHI Conference on Human Factors in Computing Systems*. ACM, Hamburg Germany, 1–15. <https://doi.org/10.1145/3544548.3581440>
- [16] Danli Luo, Jianzhe Gu, Fang Qin, Guanyun Wang, and Lining Yao. 2020. E-seed: Shape-Changing Interfaces that Self Drill. In *Proceedings of the 33rd Annual ACM Symposium on User Interface Software and Technology*. ACM, Virtual Event USA, 45–57. <https://doi.org/10.1145/3379337.3415855>
- [17] Ioanna Mitropoulou, Mathias Bernhard, and Benjamin Dillenburger. 2020. Print Paths Key-framing: Design for non-planar layered robotic FDM printing. In *Symposium on Computational Fabrication*. ACM, Virtual Event USA, 1–10. <https://doi.org/10.1145/3424630.3425408>
- [18] Mako Miyatake, Koya Narumi, Yuji Sekiya, and Yoshihiro Kawahara. 2021. Flower Jelly Printer: Slit Injection Printing for Parametrically Designed Flower Jelly. In *Proceedings of the 2021 CHI Conference on Human Factors in Computing Systems*. ACM, Yokohama Japan, 1–10. <https://doi.org/10.1145/3411764.3445346>
- [19] Martin Nisser, Christina Chen Liao, Yuchen Chai, Aradhana Adhikari, Steve Hodges, and Stefanie Mueller. 2021. LaserFactory: A Laser Cutter-based Electromechanical Assembly and Fabrication Platform to Make Functional Devices & Robots. In *Proceedings of the 2021 CHI Conference on Human Factors in Computing Systems*. ACM, Yokohama Japan, 1–15. <https://doi.org/10.1145/3411764.3445692>
- [20] Yuta Noma, Koya Narumi, Fuminori Okuya, and Yoshihiro Kawahara. 2020. Pop-up Print: Rapidly 3D Printing Mechanically Reversible Objects in the Folded State. In *Proceedings of the 33rd Annual ACM Symposium on User Interface Software and Technology*. ACM, Virtual Event USA, 58–70. <https://doi.org/10.1145/3379337.3415853>
- [21] NomeUn. 2023. *Non planar 3d printed Velcro*. Printables. <https://www.printables.com/model/549560-non-planar-3d-printed-velcro>
- [22] Jifei Ou, Gershon Dublon, Chin-Yi Cheng, Felix Heibeck, Karl Willis, and Hiroshi Ishii. 2016. Cillia: 3D Printed Micro-Pillar Structures for Surface Texture, Actuation and Sensing. In *Proceedings of the 2016 CHI Conference on Human Factors in Computing Systems*. ACM, San Jose California USA, 5753–5764. <https://doi.org/10.1145/2858036.2858257>
- [23] Eujin Pei, Jinsong Shen, and Jennifer Watling. 2015. Direct 3D printing of polymers onto textiles: experimental studies and applications. *Rapid Prototyping Journal* 21, 5 (Aug. 2015), 556–571. <https://doi.org/10.1108/RPJ-09-2014-0126>
- [24] Huaishu Peng, Jennifer Mankoff, Scott E. Hudson, and James McCann. 2015. A Layered Fabric 3D Printer for Soft Interactive Objects. In *Proceedings of the 33rd Annual ACM Conference on Human Factors in Computing Systems (CHI '15)*. Association for Computing Machinery, New York, NY, USA, 1789–1798. <https://doi.org/10.1145/2702123.2702327>
- [25] Huaishu Peng, Rundong Wu, Steve Marschner, and François Guimbretière. 2016. On-The-Fly Print: Incremental Printing While Modelling. In *Proceedings of the 2016 CHI Conference on Human Factors in Computing Systems*. ACM, San Jose California USA, 887–896. <https://doi.org/10.1145/2858036.2858106>
- [26] Franklin Pezutti-Dyer and Leah Buechley. 2022. Extruder-Turtle: A Library for 3D Printing Delicate, Textured, and Flexible Objects. In *Sixteenth International Conference on Tangible, Embedded, and Embodied Interaction*. ACM, Daejeon Republic of Korea, 1–9. <https://doi.org/10.1145/3490149.3501312>
- [27] Michael L. Rivera and Scott E. Hudson. 2019. Desktop Electrospinning: A Single Extruder 3D Printer for Producing Rigid Plastic and Electrospun Textiles. In *Proceedings of the 2019 CHI Conference on Human Factors in Computing Systems (CHI '19)*. Association for Computing Machinery, New York, NY, USA, 1–12. <https://doi.org/10.1145/3290605.3300434>
- [28] Madlaina Signer, Alexandra Ion, and Olga Sorkine-Hornung. 2021. Developable Metamaterials: Mass-fabricable Metamaterials by Laser-Cutting Elastic Structures. In *Proceedings of the 2021 CHI Conference on Human Factors in Computing Systems*. ACM, Yokohama Japan, 1–13. <https://doi.org/10.1145/3411764.3445666>
- [29] Lingyun Sun, Jiaji Li, Yu Chen, Yue Yang, Ye Tao, Guanyun Wang, and Lining Yao. 2020. 4DTexture: A Shape-Changing Fabrication Method for 3D Surfaces with Texture. In *Extended Abstracts of the 2020 CHI Conference on Human Factors in Computing Systems (CHI EA '20)*. Association for Computing Machinery, New York, NY, USA, 1–7. <https://doi.org/10.1145/3334480.3383053>
- [30] Lingyun Sun, Jiaji Li, Junzhe Ji, Deying Pan, Mingming Li, Kuangqi Zhu, Yitao Fan, Yue Yang, Ye Tao, and Guanyun Wang. 2022. X-Bridges: Designing Tunable Bridges to Enrich 3D Printed Objects' Deformation and Stiffness. In *Proceedings of the 35th Annual ACM Symposium on User Interface Software and Technology*. ACM, Bend OR USA, 1–12. <https://doi.org/10.1145/3526113.3545710>
- [31] Lingyun Sun, Deying Pan, Yuyang Zhang, Hongyi Hu, Junzhe Ji, Yue Tao, Shanghua Lou, Boyi Lian, Yitao Fan, Ye Tao, and Guanyun Wang. 2024. Touch-n-Go: Designing and Fabricating Touch Fastening Structures by FDM 3D Printing. In *Proceedings of the CHI Conference on Human Factors in Computing Systems*. ACM, Honolulu HI USA, 1–14. <https://doi.org/10.1145/3613904.3642906>
- [32] Haruki Takahashi and Jeeun Kim. 2019. 3D Pen + 3D Printer: Exploring the Role of Humans and Fabrication Machines in Creative Making. In *Proceedings of the 2019 CHI Conference on Human Factors in Computing Systems*. ACM, Glasgow Scotland UK, 1–12. <https://doi.org/10.1145/3290605.3300525>

- [33] Haruki Takahashi and Jeeun Kim. 2019. 3D Printed Fabric: Techniques for Design and 3D Weaving Programmable Textiles. In *Proceedings of the 32nd Annual ACM Symposium on User Interface Software and Technology*. ACM, New Orleans LA USA, 43–51. <https://doi.org/10.1145/3332165.3347896>
- [34] Haruki Takahashi and Jeeun Kim. 2022. Designing a Hairy Haptic Display using 3D Printed Hairs and Perforated Plates. In *Adjunct Proceedings of the 35th Annual ACM Symposium on User Interface Software and Technology*. ACM, Bend OR USA, 1–3. <https://doi.org/10.1145/3526114.3558655>
- [35] Haruki Takahashi and Homei Miyashita. 2017. Expressive Fused Deposition Modeling by Controlling Extruder Height and Extrusion Amount. In *Proceedings of the 2017 CHI Conference on Human Factors in Computing Systems*. ACM, Denver Colorado USA, 5065–5074. <https://doi.org/10.1145/3025453.3025933>
- [36] Ye Tao, Yu Chen, Jian Fang, Jinpeng Lin, Jingchun Geng, Ziqi Fang, Cejun Chen, Cheng Yang, Fan Zhang, Lingyun Sun, and Guanyun Wang. 2021. infOrigami: A Computer-aided Design Method for Introducing Traditional Perforated Boneless Lantern Craft to Everyday Interfaces. In *Adjunct Proceedings of the 34th Annual ACM Symposium on User Interface Software and Technology (UIST '21 Adjunct)*. Association for Computing Machinery, New York, NY, USA, 55–59. <https://doi.org/10.1145/3474349.3480228>
- [37] Ye Tao, Shuhong Wang, Junzhe Ji, Linlin Cai, Hongmei Xia, Zhiqi Wang, Jinghai He, Yitao Fan, Shengzhang Pan, Jinghua Xu, Cheng Yang, Lingyun Sun, and Guanyun Wang. 2023. 4Doodle: 4D Printing Artifacts Without 3D Printers. In *Proceedings of the 2023 CHI Conference on Human Factors in Computing Systems (CHI '23)*. Association for Computing Machinery, New York, NY, USA, 1–16. <https://doi.org/10.1145/3544548.3581321>
- [38] TeachingTech. 2023. *Parametric 3D printable velcro*. Printables. <https://www.printables.com/model/568587-parametric-3d-printable-velcro>
- [39] Cesar Torres, Tim Campbell, Neil Kumar, and Eric Paulos. 2015. HapticPrint: Designing Feel Aesthetics for Digital Fabrication. In *Proceedings of the 28th Annual ACM Symposium on User Interface Software & Technology*. ACM, Charlotte NC USA, 583–591. <https://doi.org/10.1145/2807442.2807492>
- [40] Guanyun Wang, Ye Tao, Ozguc Bertug Capunaman, Humphrey Yang, and Lining Yao. 2019. A-line: 4D Printing Morphing Linear Composite Structures. In *Proceedings of the 2019 CHI Conference on Human Factors in Computing Systems*. ACM, Glasgow Scotland UK, 1–12. <https://doi.org/10.1145/3290605.3300656>
- [41] Guanyun Wang, Humphrey Yang, Zeyu Yan, Nurcan Geceer Ulu, Ye Tao, Jianzhe Gu, Levent Burak Kara, and Lining Yao. 2018. 4DMesh: 4D Printing Morphing Non-Developable Mesh Surfaces. In *Proceedings of the 31st Annual ACM Symposium on User Interface Software and Technology*. ACM, Berlin Germany, 623–635. <https://doi.org/10.1145/3242587.3242625>
- [42] Guanyun Wang, Kuangqi Zhu, Lingchuan Zhou, Mengyan Guo, Haotian Chen, Zihan Yan, Deying Pan, Yue Yang, Jiayi Li, Jiang Wu, Ye Tao, and Lingyun Sun. 2023. PneuFab: Designing Low-Cost 3D-Printed Inflatable Structures for Blow Molding Artifacts. In *Proceedings of the 2023 CHI Conference on Human Factors in Computing Systems (CHI '23)*. Association for Computing Machinery, New York, NY, USA, 1–17. <https://doi.org/10.1145/3544548.3580923>
- [43] Zhiqi Wang, Linlin Cai, Xinbei Jiang, Jiayi Li, Junzhe Ji, Ting Zhang, Ye Tao, and Guanyun Wang. 2023. 4DCurve: A Shape-Changing Fabrication Method Based on Curved Paths with a 3D Printing Pen. In *Extended Abstracts of the 2023 CHI Conference on Human Factors in Computing Systems (CHI EA '23)*. Association for Computing Machinery, New York, NY, USA, 1–7. <https://doi.org/10.1145/3544549.3585831>
- [44] Xin Yan, Lin Lu, Andrei Sharf, Xing Yu, and Yulu Sun. 2021. Man-made by Computer: On-the-Fly Fine Texture 3D Printing. In *Symposium on Computational Fabrication*. ACM, Virtual Event USA, 1–10. <https://doi.org/10.1145/3485114.3485119>
- [45] Zeyu Yan, Jiasheng Li, Zining Zhang, and Huaishu Peng. 2024. SolderlessPCB: Reusing Electronic Components in PCB Prototyping through Detachable 3D Printed Housings. In *Proceedings of the CHI Conference on Human Factors in Computing Systems*. ACM, Honolulu HI USA, 1–17. <https://doi.org/10.1145/3613904.3642765>
- [46] Zeyu Yan, Anup Sathya, Sahra Yusuf, Jyh-Ming Lien, and Huaishu Peng. 2022. Fibercuit: Prototyping High-Resolution Flexible and Kirigami Circuits with a Fiber Laser Engraver. In *Proceedings of the 35th Annual ACM Symposium on User Interface Software and Technology*. ACM, Bend OR USA, 1–13. <https://doi.org/10.1145/3526113.3545652>
- [47] Humphrey Yang, Danli Luo, Kuanren Qian, and Lining Yao. 2021. Freeform Fabrication of Fluidic Edible Materials. In *Proceedings of the 2021 CHI Conference on Human Factors in Computing Systems*. ACM, Yokohama Japan, 1–10. <https://doi.org/10.1145/3411764.3445097>
- [48] Yue Zhang, Zhenyuan Wang, Jinhui Zhang, Guihua Shan, and Dong Tian. 2023. A survey of immersive visualization: Focus on perception and interaction. *Visual Informatics* 7, 4 (Dec. 2023), 22–35. <https://doi.org/10.1016/j.visinf.2023.10.003>